

FABP4-Cre Mediated Expression of Constitutively Active ChREBP Protects Against Obesity, Fatty Liver, and Insulin Resistance

Alli M. Nuotio-Antar, Naravat Pongvarin, Ming Li, Michael Schupp, Mahmoud Mohammad, Sarah Gerard, Fang Zou, and Lawrence Chan

Diabetes and Endocrinology Research Center (A.M.N.-A., N.P., M.L., L.C.), Department of Medicine, and Children's Nutrition Research Center (A.M.N.-A., M.M., S.G., F.Z.), Department of Pediatrics, Baylor College of Medicine, Houston, Texas 77030; and Charité University School of Medicine (M.S.), Institute of Pharmacology, Center for Cardiovascular Research, 10115 Berlin, Germany

Carbohydrate response element binding protein (ChREBP) regulates cellular glucose and lipid homeostasis. Although ChREBP is highly expressed in many key metabolic tissues, the role of ChREBP in most of those tissues and the consequent effects on whole-body glucose and lipid metabolism are not well understood. Therefore, we generated a transgenic mouse that overexpresses a constitutively active ChREBP isoform under the control of the fatty acid binding protein 4-Cre-driven promoter (FaChOX). Weight gain was blunted in male, but not female, FaChOX mice when placed on either a normal chow diet or an obesogenic Western diet. Respiratory exchange ratios were increased in Western diet-fed FaChOX mice, indicating a shift in whole-body substrate use favoring carbohydrate metabolism. Western diet-fed FaChOX mice showed improved insulin sensitivity and glucose tolerance in comparison with controls. Hepatic triglyceride content was reduced in Western diet-fed FaChOX mice in comparison with controls, suggesting protection from fatty liver. Epididymal adipose tissue exhibited differential expression of genes involved in differentiation, browning, metabolism, lipid homeostasis, and inflammation between Western diet-fed FaChOX mice and controls. Our findings support a role for ChREBP in modulating adipocyte differentiation and adipose tissue metabolism and inflammation as well as consequent risks for obesity and insulin resistance. (*Endocrinology* 156: 4020–4032, 2015)

Carbohydrate response element binding protein (ChREBP) is a transcription factor that is known to be expressed as α and β alternatively spliced isoforms, of which the α -isoform is activated in a glucose-dependent manner (1–6). Activation results in the nuclear translocation of ChREBP-Max-like protein (Mlx) heterodimers, and subsequent DNA binding to carbohydrate response elements initiates the transcription of genes in the glycolytic and de novo lipogenic pathways (7–11). The role of ChREBP β is hypothesized to be similar to that of ChREBP α , although activation of the β -isoform appears to be constitutive and independent of glucose concentra-

tion (2). ChREBP α expression levels are highest in tissues that regulate systemic glucose and lipid homeostasis, such as duodenum, liver, skeletal muscle, and white and brown adipose tissue depots (12).

Initial research on ChREBP focused on the role of the α -isoform in hepatocyte metabolism, in which it was originally implicated in the pathogenesis of fatty liver in genetically induced obese ob/ob mice (13, 14). However, findings from another study indicate that ChREBP-mediated increases in Scd1 $\Delta 9$ -desaturase activity in liver may generate lipid species that are metabolically beneficial when mice are fed an obesogenic high-fat diet (15). Studies

ISSN Print 0013-7227 ISSN Online 1945-7170

Printed in USA

Copyright © 2015 by the Endocrine Society

Received March 3, 2015. Accepted August 3, 2015.

First Published Online August 6, 2015

For related article see page 4008

Abbreviations: BAT, brown adipose tissue; caChREBP, constitutively active isoform of ChREBP; ChREBP, carbohydrate response element binding protein; eGFP, enhanced green fluorescent protein; EWAT, epididymal WAT; FABP4, fatty acid binding protein 4; FaChOX, FABP4-Cre; eGFP^{lox/wt}-caChREBP; GLUT4, glucose transporter 4; IWAT, inguinal WAT; Mlx, Max-like protein; NEFA, nonesterified fatty acid; PPAR, peroxisomal proliferator-activated receptor; RER, respiratory exchange ratio; SIRT1, sirtuin 1; WAT, white adipose tissue.

in pancreatic β -cells have shown that ChREBP activates glycolytic and lipogenic genes, which, in turn, may affect processes as diverse as chromatin remodeling, glucotoxicity, cell differentiation, metabolism, and proliferation in different nutritional contexts (16–22). More recently, ChREBP^{-/-} mice challenged with an obesogenic Western diet were shown to exhibit increased intestinal lipid absorption, and ChREBP-induced glycolytic activity has been implicated in the modulation of proglucagon expression in intestinal L cells, suggesting that ChREBP activity may impact whole-body metabolism via its function in cells of the gastrointestinal tract (23, 24).

Although ChREBP is highly expressed in both brown and white adipose tissues, ChREBP expression has been shown to be induced during differentiation of 3T3-L1 cells in a glucose-dependent manner, and ChREBP expression in white adipose tissue (WAT) is regulated by nutritional status, to date the effects of ChREBP activity in adipose tissues have not been directly studied (2, 12, 25). Mice that are globally deficient in ChREBP (ChREBP^{-/-}) present with decreased brown adipose tissue (BAT) and WAT weights, suggesting that ChREBP may play a role in adipogenesis (12, 14). ChREBP^{-/-} mice become hypothermic when fed high-fructose or high-sucrose diets and exhibit mild hypothermia when fed a high-fat diet, strongly suggesting a role for ChREBP in thermogenesis (12). In the context of diet-induced obesity, adipose tissue-specific overexpression of GLUT4 has been shown to confer insulin-sensitizing effects that are abolished when mice are placed on a ChREBP^{-/-} background (2). Furthermore, expression of both isoforms of *ChREBP* in sc and omental WAT depots from humans inversely correlates with a degree of obesity and insulin resistance, and bariatric weight loss is associated with increased lipogenesis in WAT (26–28). Although studies using ChREBP^{-/-} mice are confounded by complete abrogation of ChREBP effects on nonadipose tissues, such as intestine, liver, and pancreatic β -cells, results from these studies suggest an important role for ChREBP activity in the modulation of adipogenesis, and adipocyte metabolism and function that may influence whole-body insulin sensitivity.

In this study, we sought to address the hypothesis that ChREBP activity in adipose tissue plays a metabolically beneficial role in the context of diet-induced obesity. We generated a novel transgenic mouse that conditionally overexpresses a constitutively active isoform of ChREBP (caChREBP) under the control of Cre recombinase (3). We report that, under conditions of diet-induced obesity, fatty acid binding protein 4 (FABP4)-Cre-mediated expression of caChREBP resulted in an increased expression of the lipogenic ChREBP target genes in WAT, reduced adiposity, improved insulin sensitivity, and diminished progres-

sion of fatty liver. Moreover, the expression pattern of the genes involved in adipocyte differentiation, browning, and inflammation indicated a substantially broader role of ChREBP on WAT metabolism and function than previously anticipated.

Materials and Methods

Mice

C57BL/6j and B6.Cg-Tg(Fabp4-cre)1Rev/J (FABP4-Cre) mice were obtained from The Jackson Laboratory. Transgenic eGFP^{fllox/wt}-caChREBP mice that carry a construct containing a floxed enhanced green fluorescent protein (eGFP) reporter and N-terminal FLAG-tagged murine caChREBP (ChREBP Δ 1–196) under the control of a composite CAG promoter that is active in all tissues were generated at the Baylor College of Medicine Genetically Engineered Mouse Core (3). Littermates resulting from heterozygous FABP4-Cre x eGFP^{fllox/wt}-caChREBP crosses were housed and bred in a pathogen-free facility under controlled temperature and lighting with free access to water and either standard chow diet (Harlan-Teklad; 2920X) or 21% milk fat, 34% sucrose Breslow Western-type diet (TestDiet 5TFH). Male mice were used throughout the study except where noted. Mice were euthanized between 6:00 AM and 12:00 PM via isoflurane inhalation followed by cervical dislocation and cardiac perfusion with 20 ml PBS to clear tissues of circulating leukocytes. All studies were conducted after the approval of protocols by the Baylor College of Medicine Institutional Animal Care and Usage Committee.

Body composition

Total fat and lean masses were measured with an Echo magnetic resonance imaging whole-body composition analyzer (Echo Medical Systems).

Indirect calorimetry, food intake, and locomotor activity

Mice were singly housed for 1 week prior to placement in metabolic chambers. They were subsequently acclimated to metabolic chambers for 24 hours prior to measurement of indirect calorimetry and food intake in the Comprehensive Laboratory Animal Monitoring System (Columbus Instruments). Data were acquired using the Comprehensive Laboratory Animal Monitoring System data eXamination Tool (Columbus Instruments). The respiratory exchange ratio (RER) and the energy expenditure were calculated as previously described (29).

Whole-body glucose homeostasis

Mice were fasted for 6 hours prior to testing. For insulin tolerance testing, 0.75 U/kg human insulin (Eli Lilly and Co) was injected into mice. For glucose tolerance testing, 2.0 g/kg dextrose (Sigma) was used for cohorts of chow diet-fed mice, and 1.5 g/kg dextrose was used for cohorts of Western diet-fed mice. For the glucose tolerance testing, blood was collected at each time point for further analysis of plasma insulin using a rat/mouse insulin ELISA kit (EMD Millipore).

In vivo lipolysis

Mice were fasted for 6 hours prior to an ip injection of 0.1 mg/kg CL-316243, a β 3-adrenergic agonist. Whole blood was collected immediately before and 15 minutes after injection via tail bleed for further analysis of plasma free fatty acids and glycerol at each time point.

Lipid quantification

Plasma cholesterol, glycerol, free fatty acids, and triglyceride concentrations were measured using a cholesterol reagent (RAICHEM), a free glycerol reagent and a glycerol standard solution (Sigma), triglycerides GPO reagent (RAICHEM), and the HR series nonesterified fatty acid (NEFA)-HR(2) (Wako Diagnostics) assays, respectively, according to the manufacturer protocols. Liver lipid content was quantified by the Lipid Subcore of the Metabolic Pathophysiology Core at the Vanderbilt University Mouse Metabolic Phenotyping Center (Nashville, Tennessee). Analysis of the fatty acid composition in perirenal WAT depots was performed as previously described (30).

WAT histology

Ten-micrometer sections of entire single depots of formalin-fixed epididymal WAT depots were stained with hematoxylin and visualized at $\times 200$ magnification under a Zeiss Axiophot light microscope. Pictures were taken with an Optronics camera using Acquire software. Individual areas of cells captured in three independent fields per section were measured using Image J version 1.47t software (National Institutes of Health, Bethesda, Maryland).

Real-time PCR

For recombination and copy-number experiments, DNA was extracted from whole BAT or WAT tissues and representative samples of other tissues using the DNeasy blood and tissue kit (QIAGEN) according to the manufacturer's protocol. For gene expression experiments, whole BAT or inguinal or epididymal WAT depots were homogenized in QIAzol lysis reagent (QIAGEN), and total RNA extraction was carried out using the RNeasy lipid tissue minikit (QIAGEN) according to the manufacturer's protocol. Washed thioglycolate-elicited peritoneal macrophages were homogenized in TRIzol reagent (Life Technologies), and total RNA extraction was carried out, followed by clean-up with the RNeasy minikit (QIAGEN) according to the manufacturer's protocols. cDNA was generated using the TaqMan reverse transcription reagents kit (Life Technologies), according to the manufacturer's protocols. Primers used for experiments quantifying DNA recombination by SYBR Green (Life Technologies) quantitative PCR were as follows: forward, 5'-TGCTGGTTATTGTGCTGTCTCA-3', and reverse, 5'-CAC-CACCCCGGTGAACA-3'. Assays-on-Demand validated primer/probe sets (Life Technologies) were used to assay for the copy number and expression of all genes except ChREBP α and ChREBP β . ChREBP α and ChREBP β expression levels were assayed using the previously described primers (2). For gene expression experiments, data were normalized to the three most stable housekeeping genes, as determined by geNorm software (Biogazelle). For BAT, these were as follows: *B2m*, *Gapdh*, and *Ppia*; for inguinal WAT they were as follows: *18S*, *Actb*, and *B2m*; epididymal WAT were as follows: *B2m*, *Actb*, and *Gapdh*;

and for macrophages they were as follows: *Gapdh*, *Ppia*, and *Tbp*.

Protein detection

Whole livers and epididymal WAT (EWAT) depots were homogenized in modified radioimmunoprecipitation assay (RIPA) or lysis buffers, and FLAG-tagged ChREBP was pulled down using the FLAG immunoprecipitation kit according to the manufacturer's protocol (Sigma-Aldrich). Samples were run on 7.5% Mini-PROTEAN TGX precast polyacrylamide gels (Bio-Rad Laboratories) and, after transfer to a polyvinylidene difluoride membrane (Bio-Rad Laboratories), were blocked and incubated with either 1:1000 NB400–135 (ChREBP; Novus Biologicals) or 1:250 M2 (FLAG; Sigma-Aldrich) primary antibodies overnight and goat 1:2000 antirabbit or 1:5000 antimouse IgG horseradish peroxidase-conjugated secondary antibodies (Santa-Cruz) according to the manufacturer's protocols. Bands were visualized with the Amersham enhanced chemiluminescence Prime Western blotting detection reagents (GE Healthcare).

Statistical analysis

Data shown are mean \pm SEM and were analyzed with GraphPad Prism version 6, using a one-way ANOVA, a repeated-measures two-way ANOVA, an unmatched two-way ANOVA, or an unpaired Student's *t* test where appropriate. Post hoc testing of ANOVA results was carried out using Sidak's multiple comparisons test. $P < .05$ was considered statistically significant.

Results

Previously we reported that the deletion of the N-terminal low glucose inhibitory domain resulted in a constitutively active mutant of ChREBP (caChREBP) (3, 16). We sought to determine the effect of caChREBP overexpression under the control of FABP4-Cre-mediated DNA recombination in vivo using a novel transgenic mouse model, FABP4-Cre;eGFP^{lox/wt}-caChREBP (FaChOX) mice in a C57BL/6 background (Figure 1A). Seven copies of the construct were detected in genomic DNA from mice transgenic for the eGFP^{lox/wt}-caChREBP construct (Figure 1B). FABP4 promoter-driven expression of Cre has been reported to occur at high levels in adipose tissues; however, ectopic expression of the recombinase has also been described for animals that carry the *Fabp4-Cre* transgene (31–34). Examination of genomic DNA in our FaChOX mice revealed significant Cre-mediated recombination in BAT, WAT, and hypothalamus but not in other tissues tested (Supplemental Figure 1).

In the EWAT, we detected a 1.5-fold increase in total ChREBP expression levels and no differences in *Chrebp* α or combined endogenous *Chrebp* α and *Chrebp* β expression levels between FaChOX mice and controls, suggesting that expression of the caChREBP transgene was responsible for the 50% increase in total *Chrebp* expression

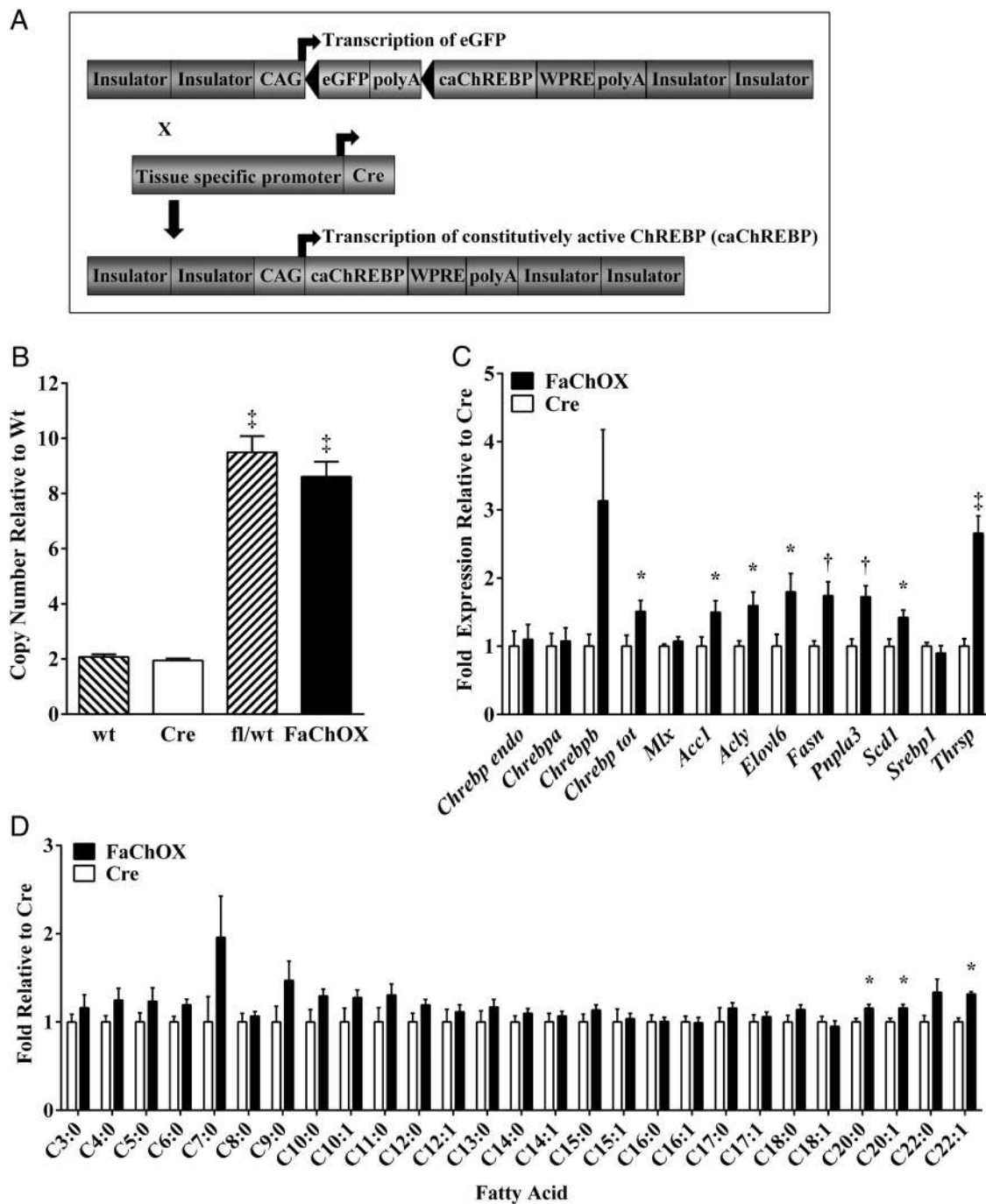


Figure 1. Overexpression of caChREBP under the control of FABP4-Cre-mediated DNA recombination results in increased target gene expression and even carbon long-chain fatty acid composition in WAT. A, Schematic of eGFP^{lox/wt}-caChREBP construct and Cre recombination in FaChOX mice. B, ChREBP copy number detected in genomic DNA of wild-type (wt), FABP4-Cre (Cre), eGFP^{lox/wt}-caChREBP(fl/wt), and FaChOX male mice (n = 5 per group). C, Gene expression of various ChREBP isoforms and lipogenic target genes, as well as *Srebp1* and binding partner *Mlx*, in EWAT taken from male Western diet-fed FaChOX vs Cre mice (n = 7–10 per group). D, Fold change in percentage composition for individual fatty acids extracted from perirenal WAT taken from male Western diet-fed mice (n = 4–6 per group). Data shown are mean ± SEM. *, P < .05 compared with Cre control; †, P < .005 compared with Cre control; ‡, P < .0001 compared with either wt or Cre control.

levels (Figure 1C). Although elevated 3-fold in FaChOX mice in comparison with controls, EWAT *ChREBPβ* expression showed substantial variability and differences did not achieve statistical significance (P = .08). Although the expression of binding partner *Mlx* did not differ,

known lipogenic ChREBP target genes *Acc1*, *Acly*, *Elavl6*, *Fasn*, *Pnpla3*, *Thrsp*, and *Scd1* were significantly up-regulated in the EWAT of FaChOX mice in comparison with controls (8, 12, 35, 36). *Srebp1* expression levels were not different between groups. Analysis of fatty acid composi-

tion revealed significantly increased C20:0, C20:1, and C22:1 long-chain fatty acids, and a trend toward increased C6:0 ($P = .05$), C10:0 ($P = .09$), and C22:0 ($P = .09$) even-chain fatty acids in the WAT taken from FaChOX mice in comparison with controls, suggesting increased synthesis, desaturation, and elongation of fatty acids in visceral WAT (Figure 1D).

We also assessed *Chrebp* and target gene expression in macrophages and other adipose depots. Consistent with a nonsignificant trend observed for Cre-mediated recombination in thioglycolate-elicited peritoneal macrophages, we were unable to detect a difference in total *Chrebp* expression between macrophages elicited from FaChOX vs littermate controls (Supplemental Figure 2A). Surprisingly, inguinal WAT (IWAT) quantitative PCR data revealed only a trend toward increased total *Chrebp* expression ($P = .07$), yet significantly up-regulated *Chrebbp*, ChREBP target gene *Thrsp*, and *Ucp1* expression levels, although no other ChREBP-target genes were differentially regulated in IWAT taken from FaChOX vs littermate controls (Supplemental Figure 2B). In BAT, total *Chrebp* expression levels were elevated 1.34-fold in FaChOX mice compared with controls, with no statistical differences for endogenous *Chrebp* or target gene expression observed, except for *Adfp* (Supplemental Figure 2C) (8). These results indicated that transgenic overexpression of caChREBP in our model was functional and physiologically relevant in vivo in EWAT and that caChREBP may only be minimally functional in macrophages, IWAT, and BAT in FaChOX mice. Furthermore, although immunoblots revealed high levels of endogenous ChREBP in EWAT and BAT depots migrating at approximately 100 kDa, caChREBP was not readily observable in whole tissue lysates, in part due to an interfering band that comigrated at approximately 75 kDa (Supplemental Figure 2D). However, after immunoprecipitation of the FLAG-tagged protein, a band migrating at the expected 75-kDa molecular mass could be observed in EWAT samples from chow diet-fed FaChOX mice (Supplemental Figure 2E).

We next addressed whether increased ChREBP activity in adipose tissue affected the progression of obesity in FaChOX mice. When placed on normal chow diet, male FaChOX mice gained less weight over time in comparison with controls, and differences in body weight gain were exacerbated when mice were placed on an obesogenic Western-type diet (Figure 2A). Although differences between genotypes did not achieve statistical significance, there was an observed trend toward decreased fat mass in male chow diet-fed FaChOX mice in comparison with fl/wt or Cre controls (Figure 2B). However, fat mass was significantly decreased in male Western diet-fed FaChOX mice in comparison with fl/wt and Cre controls. Lean mass

did not differ between groups on either diet (Figure 2B). Consistent with these findings, BAT and EWAT depot weights mirrored the differences observed for total body fat mass between groups (Table 1). Interestingly, histological examination of EWAT revealed a greater proportion of small adipocytes and a 36% increase in the number of adipocytes per field for chow diet-fed FaChOX mice in comparison with controls (Figure 2, C and D). When mice were challenged with obesogenic Western diet, adipocyte size distribution shifted to favor greater numbers of larger-sized cells and resulted in 41% and 53% fewer adipocytes counted per field for Cre and FaChOX mice, respectively, in comparison with chow diet-fed mice. Although neither adipocyte size distribution nor number of adipocytes per field differed between Western diet-fed FaChOX and Cre mice, FaChOX mice had reduced epididymal fat pad weights, suggesting that FaChOX adipocytes were larger per unit mass (Table 1). Taken together, our data indicate that FABP4-Cre-mediated overexpression of caChREBP results in reduced WAT mass that is independent of effects on adipocyte size in the context of obesity.

Female cohorts displayed a milder phenotype than male mice (Supplemental Figure 3 and Supplemental Table 1), enabling matching by body weight and lean mass between genotypes for indirect calorimetry experiments. Although effects of dietary manipulation were apparent, indirect calorimetry revealed no significant differences in energy expended between female FaChOX vs Cre and fl/wt controls fed either diet, consistent with lack of observable differences in body weights between genotypes (Figure 3A). Ambulatory activity did not differ between female FaChOX mice and controls on either diet (data not shown). There was a significant increase in caloric intake between chow vs Western diet-fed mice; however, neither total daily energy intake nor feeding pattern was different between groups of mice fed either diet (Figure 3B and data not shown). Western diet feeding resulted in significantly depressed RER for all groups of mice (Figure 3C). Notably, total, diurnal, and nocturnal RER were significantly increased in Western diet-fed FaChOX mice in comparison with controls, indicating preferential oxidation of carbohydrates over fatty acids (Figure 3, C–E). Thus, our data reveal a significant shift in whole-body metabolism in Western diet-fed FaChOX mice, in comparison with controls, even when significant differences in body weight, lean body mass, and energy expenditure are not observable.

We next examined whether glucose homeostasis is altered in FaChOX mice. When challenged with an ip glucose injection, blood glucose excursions did not differ between FaChOX mice and controls for each diet study

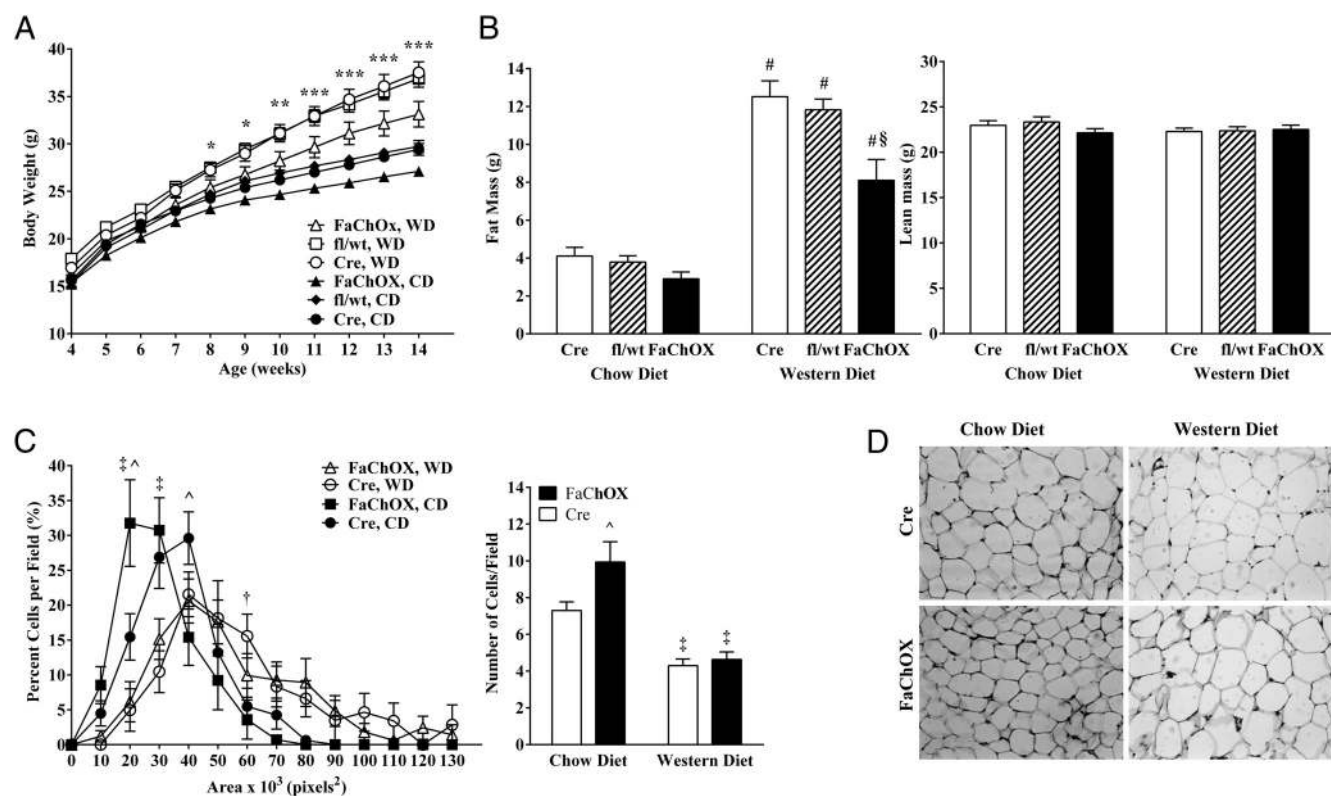


Figure 2. FaChOX mice are protected from diet-induced obesity. A, Body weight over time for male Cre, fl/wt, and FaChOX mice placed on either normal chow (CD) or Western diet (WD) for 10 weeks ($n = 12-15$ per group). B, Total fat and lean mass for male Cre, fl/wt, and FaChOX mice after 10 weeks of normal chow or Western diet feeding ($n = 12-15$ per group). C, Adipocyte size distribution and number of adipocytes per field for EWAT taken from male FaChOX vs Cre mice after normal chow or Western diet feeding for 10 weeks ($n = 9-10$ per group). D, Representative sections of EWAT from one mouse from each of the male Cre and FaChOX groups fed either chow or Western diet for 10 weeks. Magnification, $\times 200$. Data shown are mean \pm SEM. *, $P < .05$ for chow diet-fed FaChOX vs fl/wt mice; **, $P < .05$ for chow diet-fed FaChOX vs fl/wt mice and Western diet-fed FaChOX vs both fl/wt and Cre mice; ***, $P < .05$ for FaChOX vs both fl/wt and Cre mice fed either normal chow or Western diets; #, $P \leq .0001$ for FaChOX, fl/wt or Cre mice fed normal chow vs Western diets; §, $P < .0005$ for Western diet-fed FaChOX vs both fl/wt and Cre mice; †, $P \leq .001$ for normal chow diet-fed FaChOX vs Cre mice; ‡, $P \leq .0001$ for chow vs Western diets for either genotype; †, $P < .05$ for Cre mice fed normal chow vs Western diets.

(Figure 4A for chow diet fed mice and Figure 4B for Western diet fed mice). However, FaChOX mice on a Western diet, but not chow diet, exhibited attenuated insulin secretion profiles in comparison with controls. Although no differences were observed for glucose clearance during insulin tolerance testing between chow diet-fed FaChOX mice and controls, insulin tolerance testing revealed that

Western diet-fed FaChOX mice were significantly more insulin sensitive than controls (Figure 4C; data not shown: differences in glucose excursion were also evident when blood glucose values were plotted as percentage of baseline glucose). Taken together, our results confirm a beneficial effect of FABP4-Cre-induced ChREBP activity on whole-body insulin sensitivity.

Table 1. Endpoint Tissue Weights and Fasting Plasma Lipids for Male Mice

	Cre, Chow Diet	FaChOX, Chow Diet	Cre, Western Diet	FaChOX, Western Diet
BAT weight, g	0.113 \pm 0.006	0.089 \pm 0.006	0.242 \pm 0.017 ^a	0.182 \pm 0.014 ^{a,b}
Epididymal WAT weight, g	0.85 \pm 0.08	0.59 \pm 0.06	2.60 \pm 0.12 ^a	2.21 \pm 0.17 ^{a,b}
Liver weight, g	1.51 \pm 0.04	1.41 \pm 0.03	2.46 \pm 0.15 ^a	1.85 \pm 0.11 ^{a,b}
Spleen weight, g	0.080 \pm 0.003	0.075 \pm 0.002	0.099 \pm 0.002 ^a	0.092 \pm 0.003 ^a
Fasting cholesterol, mg/dL	140 \pm 11	134 \pm 8	222 \pm 9 ^a	194 \pm 10 ^a
Fasting triglycerides, mg/dL	58 \pm 4	56 \pm 2	49 \pm 2	48 \pm 1

Tissues ($n = 15-17$ per group) were dissected from ad libitum-fed mice, and plasma lipids ($n = 9-14$ per group) were measured in 6-hour-fasted mice at the end of the study. Data shown are mean \pm SEM.

^a $P < .01$ compared with chow diet mice of the same genotype.

^b $P < .05$ compared with Cre control.

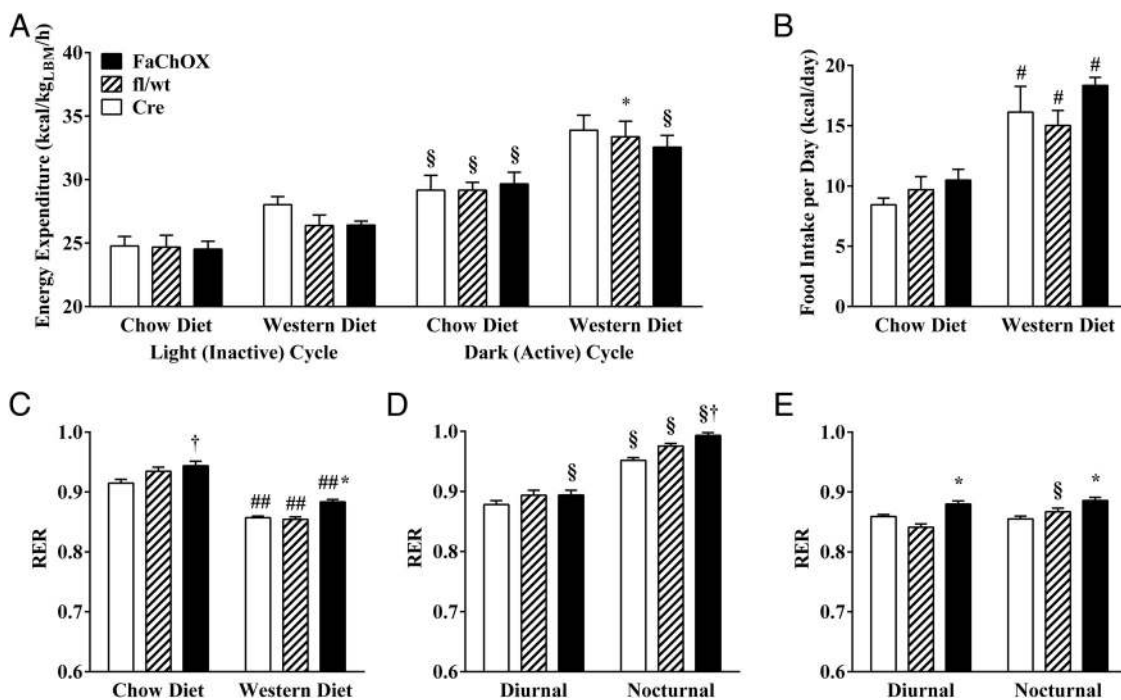


Figure 3. Respiratory exchange ratio is increased for Western diet-fed FaChOX mice in comparison with controls, indicating a shift in whole-body metabolism favoring carbohydrate oxidation. A, Energy expenditure during light and dark cycles for weight- and lean mass-matched female mice fed either chow or Western diets. B, Total daily energy intake for female mice. C, Average daily RER for chow diet vs Western diet-fed female mice. Average diurnal or nocturnal RER for female chow diet- (D) or Western diet-fed (E) mice ($n = 5-8$ per group). Data shown are mean \pm SEM. *, $P < .05$ for chow diet-fed FaChOX vs Cre or fl/wt mice within same treatment group; †, $P < .002$ for FaChOX vs Cre mice within same treatment group; #, $P < .05$ for Cre chow vs Western diet fed mice; ##, $P < .0001$ for Cre chow vs Western diet-fed mice; §, $P < .01$ for nocturnal (dark cycle) vs diurnal (light cycle) measurements.

Because insulin resistance is associated with dyslipidemia and fatty liver, we analyzed plasma and liver lipid levels. Fasting plasma cholesterol levels were increased, and triglyceride levels did not significantly differ between Western diet-fed mice compared with chow diet-fed mice (Table 1). However, consistent with a potential effect of insulin resistance on basal adipocyte lipolysis, fasting plasma NEFA levels were elevated in Western diet-fed Cre mice in comparison with chow diet-fed Cre mice but did not differ between groups after β_3 -adrenergic receptor stimulation with CL-316243 (Figure 4D). These trends were mirrored by glycerol levels before and after CL-316243 stimulation, although differences between groups at each time point did not achieve significance. Under conditions of Western diet feeding, there was no significant effect of caChREBP on fasting cholesterol or triglyceride levels, although cholesterol levels were modestly reduced by 13% for FaChOX mice ($P = .07$; Table 1). Basal circulating fasting NEFA levels were lower in Western diet-fed FaChOX mice compared with Cre controls, and this trend was observed for basal glycerol levels, although the differences between the two Western diet-fed groups did not achieve significance (Figure 4D). These results suggest a mild rescue effect of FABP4-induced caChREBP overexpression on circulating lipids that are frequently found

to be elevated in the context of diet-induced obesity and insulin resistance.

In liver, free fatty acid, cholesteryl ester, and triglyceride concentrations were increased, whereas phospholipid concentrations were decreased, with obesogenic Western diet feeding, consistent with previous observations (Figure 4E) (37). In keeping with other observed metabolically protective effects of FABP4-Cre-mediated overexpression of caChREBP in the context of diet-induced obesity, hepatic triglyceride content was reduced by 27% and phospholipid content increased by 24% in Western diet-fed FaChOX mice compared with controls. In summary, these data indicate a protective role for FABP4-induced caChREBP overexpression in the context of obesity-associated fatty liver disease but not dyslipidemia.

Glucose-induced ChREBP transcriptional activity is well established to up-regulate the expression of select glycolytic and lipogenic genes as well as modulate genes involved in a variety of other processes (Figure 1C) (1, 6–11, 38). Despite the fact that ChREBP is highly expressed in adipose tissues, to date, the effects of ChREBP activity on gene expression in adipose tissue have not been directly studied (12). Therefore, we next examined the effects of caChREBP overexpression on gene expression in adipose tissue in FaChOX mice. Expression levels of genes that are

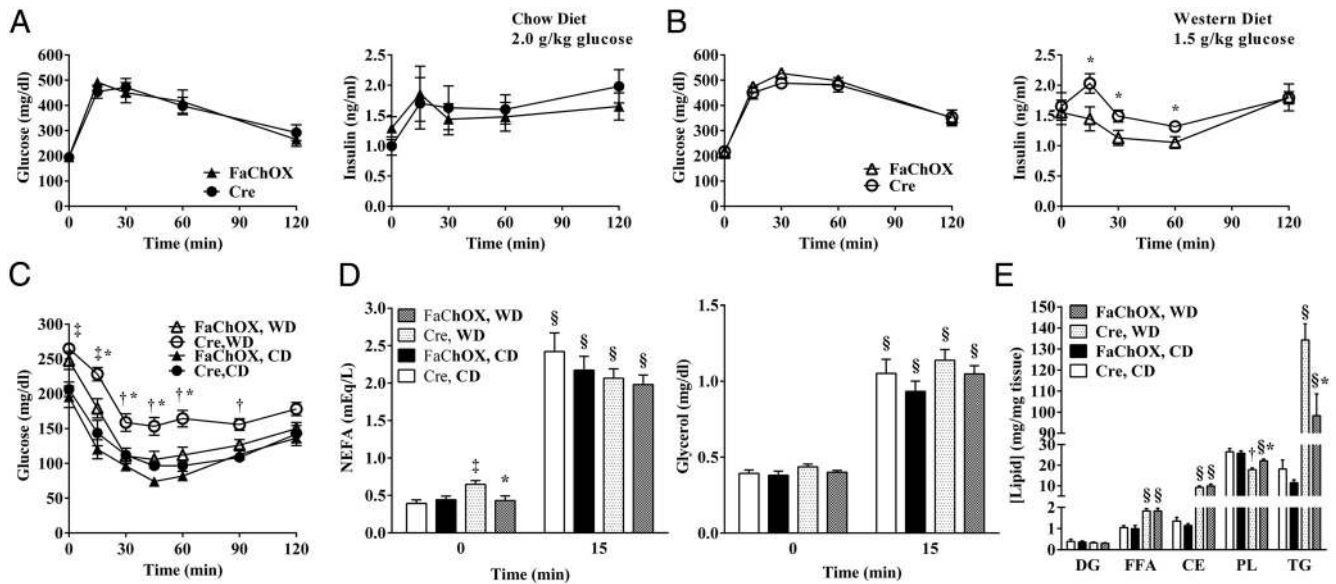


Figure 4. Western diet-fed FaChOX mice exhibit improvements in whole-body glucose homeostasis, basal lipolysis, and hepatosteatosis. A, Blood glucose and plasma insulin curves for 10-week chow diet-fed male FaChOX and Cre mice immediately prior to and post-ip injection of 2.0 g/kg dextrose ($n = 9-10$ per group). B, Blood glucose and plasma insulin curves for 10-week Western diet-fed male FaChOX and Cre mice immediately prior to and post-ip injection of 1.5 g/kg dextrose ($n = 11-14$ per group). C, Blood glucose clearance curves for 10-week chow (CD)- or Western (WD) diet-fed male FaChOX and Cre mice immediately prior to and post-ip injection of 0.75 U/kg insulin ($n = 6-8$ per group for chow diet; $n = 9-11$ per group for Western diet). D, Fasting plasma NEFA and glycerol levels immediately before and after stimulation with CL-316243 ($n = 5-7$ for male chow diet fed groups; $n = 9-10$ for male Western diet fed groups). E, Hepatic lipid levels after 10 weeks of chow or Western diet feeding ($n = 6$ for male chow diet fed groups; $n = 10$ for Western male diet fed groups). CE, cholesteryl ester; DG, diglyceride; FFA, free fatty acid; PL, phospholipid; TG, triglyceride. Data shown are mean \pm SEM. *, $P < .05$ for Western diet-fed FaChOX vs Cre mice; †, $P < .05$ for Western diet-fed Cre vs all other groups of mice; ‡, $P < .01$ for chow vs Western diet-fed mice by genotype; §, $P < .0001$ for 0 vs 15 minute time points for each group.

up-regulated during adipocyte differentiation, *Adipor2*, *Cebpa*, *Fabp4*, *Pparg2*, and *Rev-Erba*, were increased in FaChOX mice (Table 2). Expression levels of genes involved in cellular lipid homeostasis, *Fsp27*, *Gpat3*, *Hsl*, *Pck1*, *Plin1*, and *Pnpla2*, and genes that regulate peroxisomal lipid modification, *Dhapat* and *Dhrs7b*, were also increased in EWAT taken from Western diet-fed FaChOX mice in comparison with controls. However, expression of another gene involved in the modification of the fatty alcohol class of lipids by peroxisomes, *Adhafs*, was decreased by 20% in FaChOX mice compared with controls. Surprisingly, we observed significantly increased expression of *Pgc1a*, *Sirt1*, *Ucp1*, and *Ucp3* in the EWAT of FaChOX mice in comparison with controls, which may indicate greater browning of WAT. Consistent with a role for ChREBP in the regulation of intracellular glucose metabolism, the expression levels of *Anxa2*, *Glut4*, and *Tkt* were increased in EWAT taken from Western diet-fed FaChOX mice. Catalase, an intracellular antioxidant enzyme associated with peroxisomes, was also up-regulated in EWAT of FaChOX mice. Finally, expression of macrophage markers *Emr1*, *Cd11c*, and, to a lesser extent, *Cd206*, as well as proinflammatory chemokine *Ccl2*, was reduced in EWAT of Western diet-fed FaChOX mice in comparison with controls. Taken together, these data sup-

port a key role for ChREBP in the modulation of adipocyte differentiation and cellular metabolism as well as WAT inflammation.

Discussion

We have generated a novel transgenic mouse model that selectively overexpresses a constitutively active isoform of ChREBP under the control of FABP4-Cre mediated DNA recombination. Overall, our results suggest more efficient lipid storage and altered use of metabolizable nutrients in visceral WAT of FaChOX mice and support a metabolically protective function for ChREBP activity in WAT in the context of obesity and obesity-associated pathologies, such as insulin resistance and fatty liver. We observed sexual dimorphism between male and female mice, with regard to severity of phenotype, suggesting that FABP4-Cre-mediated *caChrebp* expression exerted only modest effects on the female metabolic phenotype, which has been shown to already be somewhat protected from obesity and insulin resistance in comparison with that exhibited by males (39). Despite the greater recombination efficiency observed for both BAT and IWAT in comparison with EWAT, the greatest effect of the transgene on target gene

Table 2. Western Diet-Fed Male FaChOX Mice Show Increased Expression of Adipocyte Differentiation, Other Lipogenic, Browning, and ChREBP and PPAR γ Target Genes in EWAT

Gene	Cre	FaChOX
Differentiation		
<i>Adipor2</i>	1.00 \pm 0.10	1.51 \pm 0.10 ^a
<i>Cebpa</i>	1.00 \pm 0.09	1.53 \pm 0.16 ^b
<i>Fabp4</i>	1.00 \pm 0.11	1.52 \pm 0.11 ^a
<i>Pparg2</i>	1.00 \pm 0.12	1.30 \pm 0.09 ^b
<i>Rev-Erba</i>	1.00 \pm 0.13	1.99 \pm 0.25 ^a
Lipid metabolism		
<i>Adhaps</i>	1.00 \pm 0.04	0.80 \pm 0.04 ^a
<i>Dhapat</i>	1.00 \pm 0.06	1.42 \pm 0.15 ^b
<i>Dhrs7b</i>	1.00 \pm 0.06	1.15 \pm 0.04 ^b
<i>Fsp27</i>	1.00 \pm 0.11	1.43 \pm 0.06 ^a
<i>Gpat3</i>	1.00 \pm 0.16	1.95 \pm 0.28 ^b
<i>Hsl</i>	1.00 \pm 0.11	1.53 \pm 0.12 ^a
<i>Pck1</i>	1.00 \pm 0.10	2.08 \pm 0.24 ^a
<i>Plin1</i>	1.00 \pm 0.08	1.62 \pm 0.17 ^b
<i>Pnpla2</i>	1.00 \pm 0.16	1.67 \pm 0.24 ^b
Browning		
<i>Pgc1a</i>	1.00 \pm 0.30	4.21 \pm 0.62 ^c
<i>Sirt1</i>	1.00 \pm 0.08	1.50 \pm 0.17 ^b
<i>Ucp1</i>	1.00 \pm 0.32	2.41 \pm 0.40 ^b
<i>Ucp3</i>	1.00 \pm 0.22	1.65 \pm 0.22 ^b
Glucose uptake		
<i>Anxa2</i>	1.00 \pm 0.10	1.30 \pm 0.07 ^b
<i>Glut4</i>	1.00 \pm 0.12	1.94 \pm 0.20 ^a
Pentose phosphate pathway		
<i>Tkt</i>	1.00 \pm 0.08	1.45 \pm 0.10 ^a
Antioxidant		
<i>Cat</i>	1.00 \pm 0.11	1.50 \pm 0.17 ^b
Inflammatory		
<i>Ccl2</i>	1.00 \pm 0.16	0.34 \pm 0.03 ^a
<i>Cd11c</i>	1.00 \pm 0.18	0.32 \pm 0.05 ^a
<i>Cd206</i>	1.00 \pm 0.09	0.78 \pm 0.05 ^b
<i>Emr1</i>	1.00 \pm 0.11	0.54 \pm 0.05 ^a

Data shown are mean \pm SEM (n = 7–10 per group).

^a P < .005 compared with Cre control.

^b P < .05 compared with Cre control.

^c P < .0005 compared with Cre control.

expression was observed in EWAT in comparison with the other two depots. IWAT exhibited intermediate expression of the transgene and its targets, whereas BAT showed the weakest expression of total *Chrebp* and induction of only one target gene of the many tested. Because BAT expresses much higher levels of both isoforms of *Chrebp* than WAT, it is possible that the incremental increase in total *Chrebp* expression observed in BAT may have been insufficient to exert a strong effect against an already high background of endogenous *Chrebp* expression (12). Furthermore, results from immunoblots suggest that caChREBP may be subject to enhanced degradation because the band for caChREBP gave a far lower signal than endogenous ChREBP and could be detected only after immunoprecipitation. It has been suggested that truncated ChREBP lacking a stabilizing 14–3–3 β binding site, which

is the case for the *caChrebp* transgene expressed by FaChOX mice, may be more susceptible to degradation (40). It remains to be determined whether the process of degradation is differentially modulated in different adipose tissue depots, but this may be a reason that recombination efficiency did not necessarily predict the effects of transgene expression in FaChOX mice.

FABP4-Cre mice have been reported to exhibit ectopic expression of Cre recombinase, increasing the possibility of extraadipose effects of floxed genetic modification on observed phenotypes (31–34). Cre-mediated DNA recombination was observed to vary between 37% and 59% in various adipose depots, as well as the hypothalamus, but did not achieve significance in other tissues tested in FaChOX mice, including thioglycolate-elicited peritoneal macrophages. Although total *Chrebp* expression was not significantly increased in that population of macrophages, the potential activity of caChREBP in the adipose tissue macrophages cannot be ruled out and may have contributed to the attenuated inflammatory response observed in EWAT taken from Western diet-fed FaChOX mice. Thus far, little is known about ChREBP activity in the hypothalamus. ChREBP^{-/-} mice bred on an ob/ob background exhibited decreased hyperphagia that may have been mediated by reduced levels of the orexigenic hypothalamic neuropeptide agouti-related peptide (AgRP), and this was associated with blunted weight gain over time observed for ob/ob-ChREBP^{-/-} mice compared with ob/ob controls (14). However, whether the observed effect on feeding behavior was directly mediated by hypothalamic ChREBP activity or was secondary to a shift in whole-body metabolism was not addressed. Consistent with results generated on the ob/ob background, more recently, ChREBP^{-/-} mice fed a Western diet were shown to exhibit blunted weight gain, which was associated with reduced food intake, in comparison with controls (24). Although we did not measure food intake for male mice, we did not observe any effect of FABP4-Cre-mediated transgenic overexpression of caChREBP on food intake in female mice. Moreover, data reported from ChREBP^{-/-} mouse studies suggest that overexpression of caChREBP in hypothalamus may promote increased food intake, which would likely promote weight gain in the context of obesity, yet such an effect on adiposity was not observed in FaChOX mice. Another possibility is that increased hypothalamic ChREBP activity may have reduced adiposity by promoting increased WAT lipolysis (41). However, thus far, our data support a modest role for caChREBP in blunting elevated basal fasting lipolytic responses observed in the context of Western diet-induced obesity and insulin resistance. Whether this blunting effect is indirect and due to insulin sensitizing effects of caChREBP or di-

rectly due to activity of neuronal or adipocyte caChREBP has not yet been determined. Furthermore, our observations do not completely rule out caChREBP effects on other hypothalamically modulated physiological processes that may impact body weight and insulin sensitivity, such as thermogenesis.

Increased ChREBP activity in WAT may have directly affected the metabolic phenotype observed for FaChOX mice. For instance, we observed an increased expression of many lipogenic genes, *Acc1*, *Acly*, *Elovl6*, *Fasn*, *Pnpla3*, *Thrsp*, and *Scd1*, as well as *Adipor2*, *Glut4*, and *Tkt*, which have previously been identified as ChREBP target genes as well as significantly increased lipid products of de novo synthesis, desaturation, and elongation pathways in the WAT of FaChOX mice (8, 12, 35). In healthy human subjects, de novo lipogenesis under conditions of excess carbohydrate feeding was calculated to result in the dissipation of 25% of the energy consumed in excess of maintenance energy (42). Increased de novo lipogenesis due to caChREBP activity may have subtly elevated whole-body energy expenditure below the threshold of detection by indirect calorimetry, promoting the leaner phenotype observed for Western diet-fed FaChOX mice, and this, in turn, may have protected against insulin resistance. Also, the direct up-regulation of *Adipor2* by caChREBP may have sensitized FaChOX adipocytes to adiponectin, thus potentially countering inflammation and altered glucose homeostasis promoted by Western diet feeding (43–45). Furthermore, a lipidomic analysis has recently revealed increased production of a novel class of antidiabetic and antiinflammatory lipids in WAT taken from transgenic mice selectively overexpressing glucose transporter-4 (GLUT4) in adipose tissue (46). Thus, it is possible that de novo lipogenic pathways modulated by ChREBP activity, downstream of Glut4-mediated glucose uptake, may play a role in the production of these insulin-sensitizing lipid species.

Pparg2, as well as many peroxisomal proliferator-activated receptor (PPAR)- γ -regulated genes, *Anxa2*, *Cat*, *Cebpa*, *Fabp4*, *Fsp27*, *Glut4*, *Gpat3*, *Hsl*, *Pck1*, *Pnpla2*, *Rev-Erba*, and *Ucp3*, were also increased in the WAT of Western diet-fed FaChOX mice (47–59). Hence, ChREBP overexpression in EWAT may have amplified PPAR γ activity in adipocytes via an increased expression of the nuclear receptor. In a paper cosubmitted with ours, Witte et al show compelling evidence that PPAR γ expression and activity are both increased under conditions of caChREBP overexpression in vitro, supporting this hypothesis. Recently findings by Lodhi et al (60) highlighted the potential for intracellular generation of endogenous PPAR γ ligands resulting from peroxisomal modification of lipid in WAT. We report here that the expression levels of two of the

genes that play a major role in this peroxisomal lipid modification pathway described by Lodhi et al, *Dhapat* and *Dhrs7b*, were up-regulated in the EWAT of Western diet-fed FaChOX mice. Additionally, we observed increased expression of *Sirt1* in FaChOX WAT, implying a potential for greater sirtuin 1 (SIRT1)-mediated deacetylation of PPAR γ that may further modulate PPAR γ activity in Western diet-fed FaChOX mice (61). Although elevated ChREBP activity has previously been reported to repress SIRT1 expression, both *Chrebp* and *Sirt1* expression levels have been observed to be down-regulated in WAT in obesity, suggesting that increased SIRT1 expression in WAT of FaChOX mice may be due to an indirect rescue effect of increased ChREBP activity in that tissue (26–28, 62–64). Thus, both PPAR γ and SIRT1 activities may have contributed to the browning of WAT, sensitized WAT to insulin, and attenuated inflammation in WAT, providing a potential mechanism through which increased ChREBP activity exerts its broad effects in our model (61, 65–68).

ChREBP expression has been shown to increase during differentiation of 3T3-L1 cells (25). Intriguingly, the expression levels of many genes up-regulated during adipocyte differentiation were increased in Western diet-fed FaChOX EWAT in comparison with controls. The FABP4-Cre-mediated modulation of gene expression was recently shown to occur in vivo in undifferentiated adipocyte progenitors present in adipose tissue depots, thus making it likely that the *caChrebp* expression in the FaChOX adipocytes occurred prior to differentiation (69). Thus, our data support a novel role for ChREBP as a driver of adipogenesis.

Chemokine (C-C motif) ligand-2 (CCL2) is a proinflammatory chemokine that is produced by both macrophages and adipocytes in the context of obesity (70). Reduced *Ccl2* expression in the WAT of FaChOX mice may have led to an attenuated Western diet-induced macrophage recruitment to EWAT, as evinced by the 46% reduction in *Emr1* expression in FaChOX EWAT in comparison with controls. Taking into consideration the decreased *Emr1* expression, the 68% reduction in proinflammatory *Cd11c* expression, in comparison with the more meager 22% reduction in proresolution *Cd206* expression, suggests preferentially attenuated recruitment of proinflammatory adipose tissue macrophages in visceral WAT taken from Western diet-fed FaChOX mice (71). However, it is possible that these effects may be at least in part modulated by FABP4-Cre-mediated *caChrebp* expression in macrophages. Nonetheless, our data indicate a beneficial effect of increased ChREBP activity with regard to adipose tissue inflammation, although the exact mechanism remains to be elucidated.

Our model of FABP4-Cre-mediated caChREBP overexpression in WAT provides novel insights into the function of ChREBP in vivo in WAT. We show for the first time that adipocyte ChREBP activity not only plays an important modulatory role in intracellular metabolism and lipid synthesis in WAT but also influences adipocyte differentiation, the browning of WAT, and WAT inflammation, ultimately affecting whole-body insulin sensitivity and ectopic lipid accumulation in the context of diet-induced obesity. Thus, adipocyte ChREBP activity plays a critical role linking adipocyte cellular metabolism with whole-body glucose homeostasis. Together with data presented by Witte et al (submitted for publication), our data strongly suggest that ChREBP activity in WAT may prove a promising target for future therapies aimed at reducing risk for obesity-associated pathologies, such as type 2 diabetes and hepatosteatosis.

Acknowledgments

We thank Drs Dennis Bier, C. Wayne Smith, and O'Brian Smith (Baylor College of Medicine, Houston, Texas) and Larry Swift (Vanderbilt University, Nashville, Tennessee) for their helpful discussions.

Address all correspondence and requests for reprints to: Lawrence Chan, MD, Alkek Building for Biomedical Research, Room R614, One Baylor Plaza, BCM185, Houston, TX 77030. E-mail: lchan@bcm.edu.

Author contributions include the following: A.M.N.-A. planned and executed the experiments, analyzed the data, and wrote the manuscript. N.P. and M.L. generated the transgenic construct. M.S. provided intellectual input and reviewed/edited the manuscript. M.M. performed the mass spectroscopic lipid analysis of the white adipose tissue. S.G. and F.Z. assisted with the quantitative PCR and adipocyte measurements. L.C. co-planned the project and edited the manuscript and is the guarantor of this work. The tissue lipid content was quantified at the Vanderbilt University Mouse Metabolic Phenotyping Center (DK59637).

Portions of the data were presented and published in two distinct abstracts of less than 400 words at the 92nd Annual Meeting of The Endocrine Society (2010) and the Annual Scientific Sessions of the American Heart Association (2012).

A.M.N.-A. was supported by Baylor College of Medicine-National Institute of Diabetes and Digestive and Kidney Diseases Pediatric Gastroenterology Postdoctoral Training Grant Award DK07664, Children's Nutrition Research Center-Eunice Kennedy Shriver National Institute of Child Health and Human Development Postdoctoral Training Grant Award HD007445, and American Heart Association Postdoctoral Fellowship Award 10POST3850002 from the South Central Affiliate. L.C. was supported by National Institutes of Health Grants HL051586 and

P30DK079638 for a Diabetes Research Center at Baylor College of Medicine.

Disclosure Summary: The authors have nothing to disclose.

References

- Dentin R, Pegorier JP, Benhamed F, et al. Hepatic glucokinase is required for the synergistic action of ChREBP and SREBP-1c on glycolytic and lipogenic gene expression. *J Biol Chem*. 2004;279:20314–20326.
- Herman MA, Peroni OD, Villoria J, et al. A novel ChREBP isoform in adipose tissue regulates systemic glucose metabolism. *Nature*. 2012;484:333–338.
- Li MV, Chang B, Imamura M, Pongvarin N, Chan L. Glucose-dependent transcriptional regulation by an evolutionarily conserved glucose-sensing module. *Diabetes*. 2006;55:1179–1189.
- Li MV, Chen W, Pongvarin N, Imamura M, Chan L. Glucose-mediated transactivation of carbohydrate response element-binding protein requires cooperative actions from conserved regions and essential trans-acting factor 14–3-3. *Mol Endocrinol*. 2008;22:1658–1672.
- Li MV, Chen W, Harmancey RN, et al. Glucose-6-phosphate mediates activation of the carbohydrate responsive protein (ChREBP). *Biochem Biophys Res Commun*. 2010;395:395–400.
- Yamashita H, Takenoshita M, Sakurai M, et al. A glucose-responsive transcription factor that regulates carbohydrate metabolism in the liver. *Proc Natl Acad Sci USA*. 2001;98:9116–9121.
- Ma L, Tsatsos NG, Towle HC. Direct role of ChREBP. Mlx in regulating hepatic glucose-responsive genes. *J Biol Chem*. 2005;280:12019–12027.
- Ma L, Robinson LN, Towle HC. ChREBP* Mlx is the principal mediator of glucose-induced gene expression in the liver. *J Biol Chem*. 2006;281:28721–28730.
- Ma L, Sham YY, Walters KJ, Towle HC. A critical role for the loop region of the basic helix-loop-helix/leucine zipper protein Mlx in DNA binding and glucose-regulated transcription. *Nucleic Acids Res*. 2007;35:35–44.
- Stoekman AK, Ma L, Towle HC. Mlx is the functional heteromeric partner of the carbohydrate response element-binding protein in glucose regulation of lipogenic enzyme genes. *J Biol Chem*. 2004;279:15662–15669.
- Thompson KS, Towle HC. Localization of the carbohydrate response element of the rat L-type pyruvate kinase gene. *J Biol Chem*. 1991;266:8679–8682.
- Iizuka K, Bruick RK, Liang G, Horton JD, Uyeda K. Deficiency of carbohydrate response element-binding protein (ChREBP) reduces lipogenesis as well as glycolysis. *Proc Natl Acad Sci USA*. 2004;101:7281–7286.
- Dentin R, Benhamed F, Hainault I, et al. Liver-specific inhibition of ChREBP improves hepatic steatosis and insulin resistance in ob/ob mice. *Diabetes*. 2006;55:2159–2170.
- Iizuka K, Miller B, Uyeda K. Deficiency of carbohydrate-activated transcription factor ChREBP prevents obesity and improves plasma glucose control in leptin-deficient (ob/ob) mice. *Am J Physiol Endocrinol Metab*. 2006;291:E358–E364.
- Benhamed F, Denechaud PD, Lemoine M, et al. The lipogenic transcription factor ChREBP dissociates hepatic steatosis from insulin resistance in mice and humans. *J Clin Invest*. 2012;122:2176–2194.
- Pongvarin N, Lee JK, Yechoor VK, et al. Carbohydrate response element-binding protein (ChREBP) plays a pivotal role in β cell glucotoxicity. *Diabetologia*. 2012;55:1783–1796.
- da Silva Xavier G, Sun G, Qian Q, Rutter GA, Leclerc I. ChREBP regulates Pdx-1 and other glucose-sensitive genes in pancreatic β -cells. *Biochem Biophys Res Commun*. 2010;402:252–257.

18. Noordeen NA, Khera TK, Sun G, et al. Carbohydrate-responsive element-binding protein (ChREBP) is a negative regulator of ARNT/HIF-1 β gene expression in pancreatic islet β -cells. *Diabetes*. 2010;59:153–160.
19. Cha-Molstad H, Saxena G, Chen J, Shalev A. Glucose-stimulated expression of Txnip is mediated by carbohydrate response element-binding protein, p300, and histone H4 acetylation in pancreatic β cells. *J Biol Chem*. 2009;284:16898–16905.
20. Boergesen M, Poulsen L, Schmidt SF, Frigerio F, Maechler P, Mandrup S. ChREBP mediates glucose repression of peroxisome proliferator-activated receptor α expression in pancreatic β -cells. *J Biol Chem*. 2011;286:13214–13225.
21. Metukuri MR, Zhang P, Basantani MK, et al. ChREBP mediates glucose-stimulated pancreatic β -cell proliferation. *Diabetes*. 2012;61:2004–2015.
22. Soggia A, Flosseau K, Ravassard P, Szinnai G, Scharfmann R, Guillemain G. Activation of the transcription factor carbohydrate-responsive element-binding protein by glucose leads to increased pancreatic β cell differentiation in rats. *Diabetologia*. 2012;55:2713–2722.
23. Trabelsi MS, Daoudi M, Prawitt J, et al. Farnesoid X receptor inhibits glucagon-like peptide-1 production by enteroendocrine L cells. *Nat Commun*. 2015;6:7629.
24. Wu W, Tsuchida H, Kato T, et al. Fat and carbohydrate in western diet contribute differently to hepatic lipid accumulation. *Biochem Biophys Res Commun*. 2015;461:681–686.
25. He Z, Jiang T, Wang Z, Levi M, Li J. Modulation of carbohydrate response element-binding protein gene expression in 3T3-L1 adipocytes and rat adipose tissue. *Am J Physiol Endocrinol Metab*. 2004;287:E424–E430.
26. Eissing L, Scherer T, Todter K, et al. De novo lipogenesis in human fat and liver is linked to ChREBP- β and metabolic health. *Nat Commun*. 2013;4:1528.
27. Hurtado del Pozo C, Vesperinas-Garcia G, Rubio MA, et al. ChREBP expression in the liver, adipose tissue and differentiated preadipocytes in human obesity. *Biochim Biophys Acta*. 2011;1811:1194–1200.
28. Kursawe R, Caprio S, Giannini C, et al. Decreased transcription of ChREBP- α/β isoforms in abdominal subcutaneous adipose tissue of obese adolescents with prediabetes or early type 2 diabetes: associations with insulin resistance and hyperglycemia. *Diabetes*. 2013;62:837–844.
29. Nuotio-Antar AM, Hachey DL, Hasty AH. Carbenoxolone treatment attenuates symptoms of metabolic syndrome and atherogenesis in obese, hyperlipidemic mice. *Am J Physiol Endocrinol Metab*. 2007;293:E1517–E1528.
30. Mohammad MA, Haymond MW. Regulation of lipid synthesis genes and milk fat production in human mammary epithelial cells during secretory activation. *Am J Physiol Endocrinol Metab*. 2013;305:E700–E716.
31. Lee KY, Russell SJ, Ussar S, et al. Lessons on conditional gene targeting in mouse adipose tissue. *Diabetes*. 2013;62:864–874.
32. Martens K, Bottelbergs A, Baes M. Ectopic recombination in the central and peripheral nervous system by aP2/FABP4-Cre mice: implications for metabolism research. *FEBS Lett*. 2010;584:1054–1058.
33. Mullican SE, Tomaru T, Gaddis CA, Peed LC, Sundaram A, Lazar MA. A novel adipose-specific gene deletion model demonstrates potential pitfalls of existing methods. *Mol Endocrinol*. 2013;27:127–134.
34. Wang ZV, Deng Y, Wang QA, Sun K, Scherer PE. Identification and characterization of a promoter cassette conferring adipocyte-specific gene expression. *Endocrinology*. 2010;151:2933–2939.
35. Dubuquoy C, Robichon C, Lasnier F, et al. Distinct regulation of adiponutrin/PNPLA3 gene expression by the transcription factors ChREBP and SREBP1c in mouse and human hepatocytes. *J Hepatol*. 2011;55:145–153.
36. Wang Y, Botolin D, Xu J, et al. Regulation of hepatic fatty acid elongase and desaturase expression in diabetes and obesity. *J Lipid Res*. 2006;47:2028–2041.
37. Desmarchelier C, Dahlhoff C, Keller S, Sailer M, Jahreis G, Daniel H. C57Bl/6 N mice on a Western diet display reduced intestinal and hepatic cholesterol levels despite a plasma hypercholesterolemia. *BMC Genomics*. 2012;13:84.
38. Ishii S, Iizuka K, Miller BC, Uyeda K. Carbohydrate response element binding protein directly promotes lipogenic enzyme gene transcription. *Proc Natl Acad Sci USA*. 2004;101:15597–15602.
39. Stubbins RE, Holcomb VB, Hong J, Nunez NP. Estrogen modulates abdominal adiposity and protects female mice from obesity and impaired glucose tolerance. *Eur J Nutr*. 2012;51:861–870.
40. Ge Q, Huang N, Wynn RM, et al. Structural characterization of a unique interface between carbohydrate response element-binding protein (ChREBP) and 14–3-3 β protein. *J Biol Chem*. 2012;287:41914–41921.
41. Bartness TJ, Liu Y, Shrestha YB, Ryu V. Neural innervation of white adipose tissue and the control of lipolysis. *Front Neuroendocrinol*. 2014;35:473–493.
42. Acheson KJ, Schutz Y, Bessard T, Anantharaman K, Flatt JP, Jequier E. Glycogen storage capacity and de novo lipogenesis during massive carbohydrate overfeeding in man. *Am J Clin Nutr*. 1988;48:240–247.
43. Wu X, Motoshima H, Mahadev K, Stalker TJ, Scalia R, Goldstein BJ. Involvement of AMP-activated protein kinase in glucose uptake stimulated by the globular domain of adiponectin in primary rat adipocytes. *Diabetes*. 2003;52:1355–1363.
44. Holland WL, Miller RA, Wang ZV, et al. Receptor-mediated activation of ceramidase activity initiates the pleiotropic actions of adiponectin. *Nat Med*. 2011;17:55–63.
45. Sell H, Dietze-Schroeder D, Eckardt K, Eckel J. Cytokine secretion by human adipocytes is differentially regulated by adiponectin, AICAR, and troglitazone. *Biochem Biophys Res Commun*. 2006;343:700–706.
46. Yore MM, Syed I, Moraes-Vieira PM, et al. Discovery of a class of endogenous mammalian lipids with anti-diabetic and anti-inflammatory effects. *Cell*. 2014;159:318–332.
47. Armoni M, Kritiz N, Harel C, et al. Peroxisome proliferator-activated receptor- γ represses GLUT4 promoter activity in primary adipocytes, and rosiglitazone alleviates this effect. *J Biol Chem*. 2003;278:30614–30623.
48. Bugge A, Siersback M, Madsen MS, Gondor A, Rougier C, Mandrup S. A novel intronic peroxisome proliferator-activated receptor γ enhancer in the uncoupling protein (UCP) 3 gene as a regulator of both UCP2 and -3 expression in adipocytes. *J Biol Chem*. 2010;285:17310–17317.
49. Cao J, Li JL, Li D, Tobin JF, Gimeno RE. Molecular identification of microsomal acyl-CoA:glycerol-3-phosphate acyltransferase, a key enzyme in de novo triacylglycerol synthesis. *Proc Natl Acad Sci USA*. 2006;103:19695–19700.
50. Deng T, Shan S, Li PP, et al. Peroxisome proliferator-activated receptor- γ transcriptionally up-regulates hormone-sensitive lipase via the involvement of specificity protein-1. *Endocrinology*. 2006;147:875–884.
51. Devine JH, Eubank DW, Clouthier DE, et al. Adipose expression of the phosphoenolpyruvate carboxykinase promoter requires peroxisome proliferator-activated receptor γ and 9-cis-retinoic acid receptor binding to an adipocyte-specific enhancer in vivo. *J Biol Chem*. 1999;274:13604–13612.
52. Fontaine C, Dubois G, Duguay Y, et al. The orphan nuclear receptor Rev-Erba is a peroxisome proliferator-activated receptor (PPAR) γ target gene and promotes PPAR γ -induced adipocyte differentiation. *J Biol Chem*. 2003;278:37672–37680.
53. Glorian M, Duplus E, Beale EG, Scott DK, Granner DK, Forest C. A single element in the phosphoenolpyruvate carboxykinase gene

- mediates thiazolidinedione action specifically in adipocytes. *Biochimie*. 2001;83:933–943.
54. Huang J, Hsia SH, Imamura T, Usui I, Olefsky JM. Annexin II is a thiazolidinedione-responsive gene involved in insulin-induced glucose transporter isoform 4 translocation in 3T3-L1 adipocytes. *Endocrinology*. 2004;145:1579–1586.
 55. Kershaw EE, Schupp M, Guan HP, Gardner NP, Lazar MA, Flier JS. PPAR γ regulates adipose triglyceride lipase in adipocytes in vitro and in vivo. *Am J Physiol Endocrinol Metab*. 2007;293:E1736–E1745.
 56. Matsusue K, Kusakabe T, Noguchi T, et al. Hepatic steatosis in leptin-deficient mice is promoted by the PPAR γ target gene Fsp27. *Cell Metab*. 2008;7:302–311.
 57. Okuno Y, Matsuda M, Kobayashi H, et al. Adipose expression of catalase is regulated via a novel remote PPAR γ -responsive region. *Biochem Biophys Res Commun*. 2008;366:698–704.
 58. Tontonoz P, Hu E, Graves RA, Budavari AI, Spiegelman BM. mPPAR γ 2: tissue-specific regulator of an adipocyte enhancer. *Genes Dev*. 1994;8:1224–1234.
 59. Tontonoz P, Hu E, Devine J, Beale EG, Spiegelman BM. PPAR γ 2 regulates adipose expression of the phosphoenolpyruvate carboxykinase gene. *Mol Cell Biol*. 1995;15:351–357.
 60. Lodhi IJ, Yin L, Jensen-Urstad AP, et al. Inhibiting adipose tissue lipogenesis reprograms thermogenesis and PPAR γ activation to decrease diet-induced obesity. *Cell Metab*. 2012;16:189–201.
 61. Qiang L, Wang L, Kon N, et al. Brown remodeling of white adipose tissue by Sirt1-dependent deacetylation of Ppar γ . *Cell*. 2012;150:620–632.
 62. Costa CS, Hammes TO, Rohden F, et al. SIRT1 transcription is decreased in visceral adipose tissue of morbidly obese patients with severe hepatic steatosis. *Obes Surg*. 2010;20:633–639.
 63. Noriega LG, Feige JN, Canto C, et al. CREB and ChREBP oppositely regulate SIRT1 expression in response to energy availability. *EMBO Rep*. 2011;12:1069–1076.
 64. Qiao L, Shao J. SIRT1 regulates adiponectin gene expression through Foxo1-C/enhancer-binding protein α transcriptional complex. *J Biol Chem*. 2006;281:39915–39924.
 65. Sugii S, Olson P, Sears DD, et al. PPAR γ activation in adipocytes is sufficient for systemic insulin sensitization. *Proc Natl Acad Sci USA*. 2009;106:22504–22509.
 66. Gillum MP, Kotas ME, Erion DM, et al. Sirt1 regulates adipose tissue inflammation. *Diabetes*. 2011;60:3235–3245.
 67. Xu C, Bai B, Fan P, et al. Selective overexpression of human SIRT1 in adipose tissue enhances energy homeostasis and prevents the deterioration of insulin sensitivity with ageing in mice. *Am J Transl Res*. 2013;5:412–426.
 68. Yoshizaki T, Milne JC, Imamura T, et al. SIRT1 exerts anti-inflammatory effects and improves insulin sensitivity in adipocytes. *Mol Cell Biol*. 2009;29:1363–1374.
 69. Shan T, Liu W, Kuang S. Fatty acid binding protein 4 expression marks a population of adipocyte progenitors in white and brown adipose tissues. *FASEB J*. 2013;27:277–287.
 70. Kanda H, Tateya S, Tamori Y, et al. MCP-1 contributes to macrophage infiltration into adipose tissue, insulin resistance, and hepatic steatosis in obesity. *J Clin Invest*. 2006;116:1494–1505.
 71. Fujisaka S, Usui I, Bukhari A, et al. Regulatory mechanisms for adipose tissue M1 and M2 macrophages in diet-induced obese mice. *Diabetes*. 2009;58:2574–2582.